VIP Methane Activation Very Important Paper

International Edition: DOI: 10.1002/anie.201412441
German Edition: DOI: 10.1002/ange.201412441

On the Role of the Electronic Structure of the Heteronuclear Oxide Cluster $[Ga_2Mg_2O_5]^{\bullet+}$ in the Thermal Activation of Methane and Ethane: An Unusual Doping Effect**

*Jilai Li, Xiao-Nan Wu, Maria Schlangen, Shaodong Zhou, Patricio González-Navarrete, Shiya Tang, and Helmut Schwarz**

Abstract: *The reactivity of the heteronuclear oxide cluster $[Ga_2Mg_2O_5]^{\bullet+}$, bearing an unpaired electron at a bridging oxygen atom ($O_b^{\bullet-}$), towards methane and ethane has been studied using Fourier transform ion cyclotron resonance mass spectrometry (FT-ICR-MS). Hydrogen-atom transfer (HAT) from both methane and ethane to the cluster ion is identified experimentally. The reaction mechanisms of these reactions are elucidated by state-of-the-art quantum chemical calculations. The roles of spin density and charge distributions in HAT processes, as revealed by theory, not only deepen our mechanistic understanding of C–H bond activation but also provide important guidance for the rational design of catalysts by pointing to the particular role of doping effects.*

C–H bond activation of methane under ambient conditions continues to attract much attention,[1] not only because of the great economic interest, but also due to the inherent scientific challenges associated with this seemingly trivial transformation.[1e,2] Well-designed, state-of-the-art mass spectrometry (MS) experiments in conjunction with quantum chemical (QC) calculations have permitted the identification of the elementary steps of methane activation at a strictly molecular level and, thus, provided mechanistic insights, which are a prerequisite for the rational design of low-molecular-weight catalysts.[1a–d]

Spin density plays a crucial role in the hydrogen-atom transfer (HAT) from methane to cluster oxides.[3] In particular, metal oxides (MOs) possessing a terminal oxygen-centered radical ($O_t^{\bullet-}$) are capable of activating even methane, the least reactive hydrocarbon.[4] In contrast, MOs containing a bridging oxygen-centered radical ($O_b^{\bullet-}$) have been found to be much less reactive; here, HAT takes place only in reactions with more reactive alkanes.[3a,4h,5] Further, the local charge distribution around the $O^{\bullet-}$ centers also influences the kinetic features of HAT.[4i,6] In addition, the HAT activation barrier correlates with the reorganization energies of the reactants required to accept and donate the hydrogen atom.[3b,6c,7]

Magnesium oxide exhibits relatively good reactivity toward methane,[8] and magnesium oxide species have served in gas-phase experiments as model systems for methane activation. For example, diatomic $[MgO]^{\bullet+}$ activates methane under thermal conditions in the gas phase,[9] while $[Mg_2O_2]^{\bullet+}$, as the most simple homonuclear cluster unit of $[MgO]^{\bullet+}$,[9,10] exhibits a much lower reactivity and is only reactive towards propane and higher alkanes.[8b,9,11] Further, it has been found that the reactivity of magnesium oxides, or of zeolites, can be enhanced upon doping with other metals.[6a,11,12] Despite extensive mechanistic studies and a good understanding of some aspects,[8b,9,11,13] controversies still exist.[14] Herein we report our combined experimental/computational findings on the reactivity of the heteronuclear $[Ga_2Mg_2O_5]^{\bullet+}$ cluster toward methane and ethane in gas phase (see the Supporting Information for details of the experimental and computational methods).

The FT-ICR mass spectra in Figure 1 show the reactions of mass-selected, thermalized $[Ga_2Mg_2O_5]^{\bullet+}$ ions ($m/z = 268$, see Supporting Information for details) with isotopomers of methane and ethane; spectra of the reactions with background impurities as well as with helium as an inert substrate have also been recorded as reference spectra. As observed in Figure 1a, the HAT product ion $[Ga_2Mg_2O_5H]^+$ is generated even when only He is introduced into the ICR cell. This reveals that $[Ga_2Mg_2O_5]^{\bullet+}$ reacts via HAT with impurities like water and hydrocarbon residues present in the ICR cell. However, HAT from ethane (Reaction (1)) can clearly be

$$[Ga_2Mg_2O_5]^{\bullet+} + C_2H_6 \rightarrow [Ga_2Mg_2O_5H]^+ + C_2H_5^{\bullet} \quad \Delta H_r = -115.8\ \mathrm{kJ\,mol^{-1}} \qquad (1)$$

identified when comparing the spectra in Figures 1a,b: the intensity of the product ion $[Ga_2Mg_2O_5H]^+$ is much higher when ethane is leaked into the ICR cell (Figure 1b) instead of only He (Figure 1a) with the same pressures applied. By

[*] Dr. J. Li, Dr. X.-N. Wu, Dr. M. Schlangen, Dr. S. Zhou, Dr. P. González-Navarrete, Dr. S. Tang, Prof. Dr. H. Schwarz
Institut für Chemie, Technische Universität Berlin
Strasse des 17. Juni 135, 10623 Berlin (Germany)
E-mail: Helmut.Schwarz@tu-berlin.de
Dr. J. Li
State Key Laboratory of Theoretical and Computational Chemistry
Institute of Theoretical Chemistry, Jilin University
Changchun 130023 (P.R. China)

[**] This research was sponsored by the Deutsche Forschungsgemeinschaft (DFG), in particular the Cluster of Excellence "Unifying Concepts in Catalysis" (coordinated by the Technische Universität Berlin and funded by the DFG), and the Fonds der Chemischen Industrie. Dr. J. Li. is grateful to "Unicat" for a postdoctoral fellowship. Dr. X.-N. Wu and Dr. P. González-Navarrete appreciate support from the Alexander von Humboldt Foundation in the form of postdoctoral research fellowships. We are grateful for helpful discussions with Dr. N. Rijs, Dr. R. Kretschmer, and Dr. T. Weiske.

Supporting information for this article is available on the WWW under http://dx.doi.org/10.1002/anie.201412441.

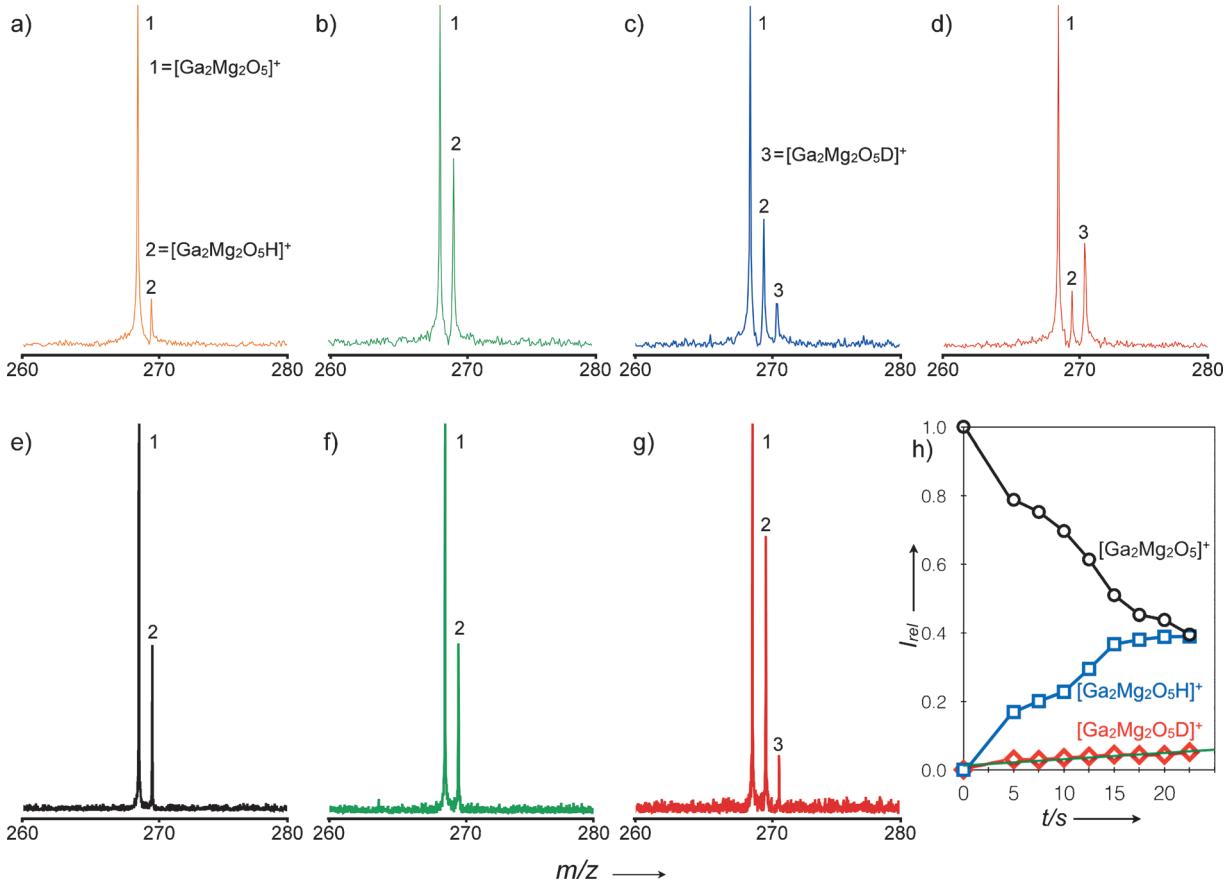

Figure 1. Mass spectra showing the reactivity of $[Ga_2Mg_2O_5]^{\bullet+}$ with a) He, b) C_2H_6, c) CH_3CD_3, and d) C_2D_6, respectively, at a pressure of 3.0×10^{-8} mbar and a reaction delay of 5 s, and with e) background air, f) CH_4, and g) CD_4 at pressures of 1.5×10^{-9}, 1.0×10^{-7}, and 2.0×10^{-7} mbar, respectively; reaction delays of 10, 10, and 20 s, respectively. The relative intensities of the reactant ion $[Ga_2Mg_2O_5]^{\bullet+}$ as well as the product ions $[Ga_2Mg_2O_5H]^+$ and $[Ga_2Mg_2O_5D]^+$ in the reaction with CD_4 as a function of the time are shown in (h). The signal $[Ga_2Mg_2O_5H]^+$ is caused by HAT from the substrate and/or from background impurities such as H_2O. See text for details.

subtracting the portion of the reactions with the background from the overall intensity of the product ion $[Ga_2Mg_2O_5H]^+$, the rate constant $k([Ga_2Mg_2O_5]^{\bullet+}/C_2H_6)$ is estimated to be 1.7×10^{-10} cm^3 molecule^{-1} s^{-1}, corresponding to a collision efficiency of 18%. The intramolecular kinetic isotope effect (KIE) derived from the $[Ga_2Mg_2O_5]^{\bullet+}/CH_3CD_3$ system (Figure 1c) amounts to 1.5.

Regarding the activity of $[Ga_2Mg_2O_5]^{\bullet+}$ towards methane, the background reactions make the evaluation of the data more difficult. Thus, when $[Ga_2Mg_2O_5]^{\bullet+}$ ions are trapped for 10 s in the ICR cell without introducing a substrate (at a background pressure of 1.5×10^{-9} mbar), $[Ga_2Mg_2O_5H]^+$ ions are observed (Figure 1e) resulting from reactions with impurities. Repeating this experiment on another day shows that the degree of background reactions is subject to large day-to-day fluctuations. When $[Ga_2Mg_2O_5]^{\bullet+}$ ions are exposed to CH_4 introduced into the reaction cell at a stationary pressure of 1.0×10^{-7} mbar (Figure 1f), the intensity of $[Ga_2Mg_2O_5H]^+$ is almost the same as in Figure 1e. Thus, HAT from methane cannot be identified unequivocally from this experiment. However, HAT from methane is clearly demonstrated in labeling experiments (Figure 1g): $[Ga_2Mg_2O_5D]^+$ ions are generated which originate from the reaction of $[Ga_2Mg_2O_5]^{\bullet+}$ with CD_4 under the elimination of $CD_3^{\bullet}$ (Reaction (2)); the composition of $[Ga_2Mg_2O_5D]^+$ has been confirmed in high-resolution measurements. Taking only the intensity of $[Ga_2Mg_2O_5D]^+$ into account and neglecting the formation of $[Ga_2Mg_2O_5H]^+$ from background reactions, the rate coefficient for Reaction (2) is estimated to be 4.0×10^{-13} cm^3 molecule^{-1} s^{-1}; this corresponds to a collision efficiency (ϕ) of 0.4%.

$$[Ga_2Mg_2O_5]^{\bullet+} + CD_4 \rightarrow [Ga_2Mg_2O_5D]^+ + CD_3^{\bullet} \quad (2)$$
$$\Delta H_r = -88.7\ \text{kJ mol}^{-1}$$

To obtain mechanistic insights in the $[Ga_2Mg_2O_5]^{\bullet+}$ mediated HAT from methane and ethane, QC calculations were carried out;[15] the corresponding potential energy surfaces (PESs) of these reactions are shown in Figure 2. The most stable structure of $[Ga_2Mg_2O_5]^{\bullet+}$ corresponds to a quasi-planar structure with the spin density unevenly distributed over the bridging oxygen atoms of the [Mg-(μ-O)$_2$Mg] moiety (Figure S1 and Figure 2, **R**). In the reaction of $[Ga_2Mg_2O_5]^{\bullet+}$ with C_2H_6, an encounter complex (EC) **1a** is formed initially from the reactants (**R** and C_2H_6); this step is exothermic by −57 kJ mol^{-1}. Subsequently, one C–H bond is

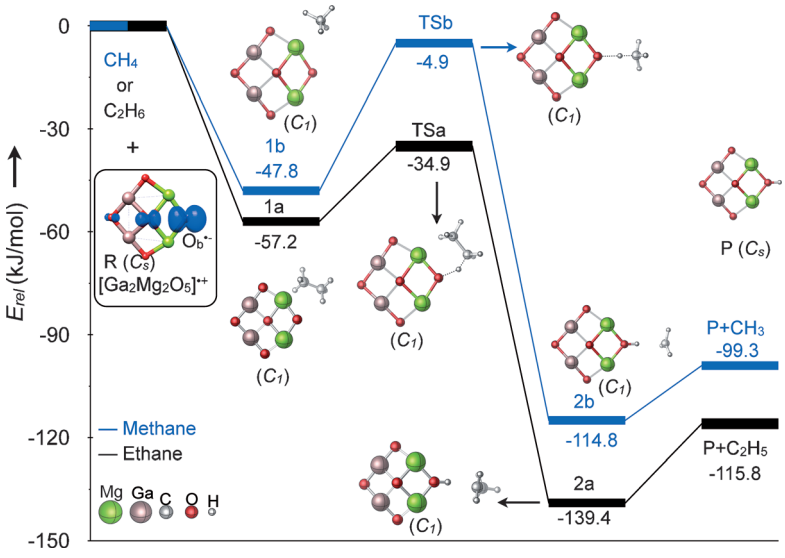

Figure 2. The potential energy surfaces (kJ mol^{-1}) and key ground-state structures involved in the reactions of the reactant $[Ga_2Mg_2O_5]^{\bullet+}$ with methane and ethane at the G4MP2-6X level of theory. The inset shows the ground-state structure of $[Ga_2Mg_2O_5]^{\bullet+}$ (C_s symmetry). The blue isosurface indicates the AIM-calculated spin density distribution.

activated and the corresponding hydrogen atom is transfered to the $O_b^{\bullet-}$ unit of **R** via transition state **TSa** which is −35 kJ mol^{-1} lower in energy than the separated reactants. This HAT process results in the formation of the association product **2a** (−139 kJ mol^{-1}), in which the ethyl radical is loosely coordinated to the cluster via the H atom of the newly formed OH group. Finally, the hydroxide product ion **P** is generated under evaporation of an ethyl radical. As shown in Figure 2, the rate-determining step corresponds to transition state **TSa** which is accessible under thermal conditions, in line with the experimental results.

As expected, and also in line with the experiments, the same mechanism as that for the reaction of $[Ga_2Mg_2O_5]^{\bullet+}$ and C_2H_6 has also been identified for the reaction of $[Ga_2Mg_2O_5]^{\bullet+}$ with CH_4. As shown in Figure 2, the corresponding rate-determining transition state **TSb** is −5 kJ mol^{-1} lower in energy than the reactants, thus indicating that this reaction is also accessible under thermal conditions. However, as the relative energy of HAT via **TSb** is 30 kJ mol^{-1} higher than that via **TSa**, the experimentally observed reaction efficiency of HAT from methane (Reaction (2)) is much lower than HAT from ethane (Reaction (1)).

In order to gain insight into the doping effect of the Ga_2O_3 unit, the reaction mechanisms of the related $[Mg_2O_2]^{\bullet+}/CH_4$ and $[Mg_2O_2]^{\bullet+}/C_2H_6$ systems were also studied computationally for comparison.[8b] While the overall mechanisms of the HAT reactions of the homonuclear magnesium oxide (Figure S2) corresponds to that calculated for the mixed oxide as described above, much higher barriers are encountered for the homonuclear magnesium oxides: HATs from methane and ethane are hampered by kinetic barriers of 21 kJ mol^{-1} and 9 kJ mol^{-1}, respectively, relative to the separated reactants $[Mg_2O_2]^{\bullet+}/CH_4$ and $[Mg_2O_2]^{\bullet+}/C_2H_6$. Further, the reaction is about 40 kJ mol^{-1} less exothermic for the $[Mg_2O_2]^{\bullet+}/C_nH_{2n+2}$ systems compared to the $[Ga_2Mg_2O_5]^{\bullet+}/C_nH_{2n+2}$ reactant pairs ($n=1,2$), respectively.

Regarding the structural features of the reaction intermediates, distinct differences are also observed for the $[Mg_2O_2]^{\bullet+}/CH_4$ and $[Ga_2Mg_2O_5]^{\bullet+}/CH_4$ systems. For example, in the reaction of $[Mg_2O_2]^{\bullet+}$ with CH_4 on going from the reactants to the HAT transition state, the two $Mg-O_b^{\bullet-}$ bonds at the reactive site of the cluster and the C–H bond of methane increase from 1.85 Å to 1.96 Å and from 1.10 Å to 1.20 Å, respectively; the O–H bond length in the transition structure amounts to 1.38 Å. In sharp contrast, in the $[Ga_2Mg_2O_5]^{\bullet+}/CH_4$ system the two $Mg-O_b^{\bullet-}$ bonds at the reactive site remain almost intact (1.94 Å to 1.93 Å), the C–H bond in transition structure **TSb** is elongated by only 0.04 Å compared to free methane, and the O–H bond with 1.59 Å is much longer than the O–H bond of the $[Mg_2O_2]^{\bullet+}/CH_4$ system (Table 1). Thus, the transition states of the $[Ga_2Mg_2O_5]^{\bullet+}/CH_4$ and $[Mg_2O_2]^{\bullet+}/CH_4$ systems correspond to early and late transition structures, respectively.[16] Moreover, the addition of the $[Ga_2O_3]$ motif to $[Mg_2O_2]^{\bullet+}$ in the $[Ga_2Mg_2O_5]^{\bullet+}$ cluster results in longer $Mg-O_b^{\bullet-}$ bond lengths (Table 1) with correspondingly lower force constants. Thus, the calculated frequencies of the $Mg-O_b^{\bullet-}$ stretching modes are $\nu_{sym}(Mg\text{-}O_b^{\bullet-}) = 340\ cm^{-1}$ for $[Mg_2O_2]^{\bullet+}$ and $\nu_{sym}(MgO_b^{\bullet-}) = 271\ cm^{-1}$ for $[Ga_2Mg_2O_5]^{\bullet+}$, respectively, indicating that the reorganization energy for the $[Ga_2Mg_2O_5]^{\bullet+}/CH_4$ system is lower than that required for $[Mg_2O_2]^{\bullet+}/CH_4$.[3a,6c] Accordingly, the barrier for the self-exchange reaction is lower for $[Ga_2Mg_2O_5]^{\bullet+}/[Ga_2Mg_2O_5H]^+$ than for the $[Mg_2O_2]^{\bullet+}/[Mg_2O_2H]^+$ system, due to smaller

Table 1: Geometric parameters of stationary points in the reactions of $[Mg_2O_2]^{\bullet+}$ and $[Ga_2Mg_2O_5]^{\bullet+}$ with methane calculated at the BMK/6-31+G(2df,p) level of theory. Bond length, [Å]; angle, [°].

	$[Mg_2O_2]^{\bullet+}$						$[Ga_2Mg_2O_5]^{\bullet+}$					
	$R_{Mg\text{-}O}$	$R_{O\text{-}H}$	$R_{C\text{-}H}$	$R_{Mg\text{-}Mg}$	$R_{O\text{-}O}$	∡O-H-C	$R_{Mg\text{-}O}$	$R_{O\text{-}H}$	$R_{C\text{-}H}$	$R_{Mg\text{-}Mg}$	$R_{O\text{-}O}$	∡O-H-C
R + CH_4	1.85	–	1.10	2.75	2.48	–	1.93	–	1.10	3.13	2.4	–
1b	1.86	3.36	1.11	2.76	2.48	109.40	1.94	2.96	1.10	3.17	2.4	109.3
TSb	1.96	1.38	1.20	2.64	2.63	178.10	1.93	1.59	1.14	3.03	2.5	177.3
2b	1.93	0.97	2.18	2.56	2.72	173.89	1.93	0.97	2.18	2.88	2.6	171.7
P + CH_3	1.94	0.96	–	2.58	2.71	–	1.93	0.96	–	2.90	2.6	–

structural changes and smaller force constants in the former system (Figure S3).

A Bader population analysis[17] has also been performed to provide even deeper insight. The AIM (Atoms in Molecules) charge of both bridging oxygen atoms is −1.279e for the homonuclear magnesium oxide $[Mg_2O_2]^{\bullet+}$, whereas the charge of the $O_b^{\bullet-}$ unit that constitutes the reactive site in $[Ga_2Mg_2O_5]^{\bullet+}$ amounts to only −0.941e (Table S1). Moreover, the spin density in $[Mg_2O_2]^{\bullet+}$ is delocalized and amounts to 0.517e on each O atom. In contrast, for $[Ga_2Mg_2O_5]^{\bullet+}$, this value increases up to 0.896e on $O_b^{\bullet}$ at the active site, while the spin density at the oxygen atom in the center of $[Ga_2Mg_2O_5]^{\bullet+}$ is reduced to 0.092e. Thus, the $[Ga_2O_3]$ fragment affects both the charge and the spin distribution of the reactive $[Mg(\mu\text{-}O_b^{\bullet})Mg]$ unit: as noted earlier,[4i,6a] increasing spin density and decreasing charge on $O_b^{\bullet-}$ favorably affect a reactive species, with the consequence that even methane can be activated. These effects are nicely demonstrated in a comparison of the spin and charge distributions at the oxygen atoms that constitute the active sites of the four oxides $[MgO]^{\bullet+}$,[9] $[Mg_2O_2]^{\bullet+}$,[8b] $[Ga_2Mg_2O_5]^{\bullet+}$, and the recently studied homonuclear cluster $[La_{10}O_{15}]^{\bullet+}$;[18] with the exception of $[Mg_2O_2]^{\bullet+}$, the three other oxides are—with different efficiencies—capable of HAT from methane at ambient conditions. The rate constants amount to 3.9×10^{-10} $cm^3 molecule^{-1} s^{-1}$ for $[MgO]^{\bullet+}$ bearing an unpaired electron at a terminal oxygen atom ($O_t^{\bullet-}$), and to 4.0×10^{-13} and 1.0×10^{-12} $cm^3 molecule^{-1} s^{-1}$ for $[Ga_2Mg_2O_5]^{\bullet+}$ and $[La_{10}O_{15}]^{\bullet+}$, respectively, bearing higher spin densities at bridging oxygen atoms. As shown in Figure 3a, the highest spin density, close to 1, is located at the terminal oxygen of $[MgO]^{\bullet+}$, whereas the lowest value of around 0.5 has been found at the bridging oxygen atoms in $[Mg_2O_2]^{\bullet+}$. Also $[Ga_2Mg_2O_5]^{\bullet+}$ and $[La_{10}O_{15}]^{\bullet+}$ exhibit spin density only at bridging instead of terminal oxygen atoms; however, the spin density at one of these bridging oxygen atoms is much higher than that calculated for $[Mg_2O_2]^{\bullet+}$ and reaches almost the spin density obtained for the $O_t^{\bullet-}$ in $[MgO]^{\bullet+}$. Since the spin density and the local charge at the oxygen atom are not independent,[1c] the same holds true for the charge distribution: as shown in Figure 3b, a less negative charge on the reactive oxygen atom is beneficial for HAT reactions.

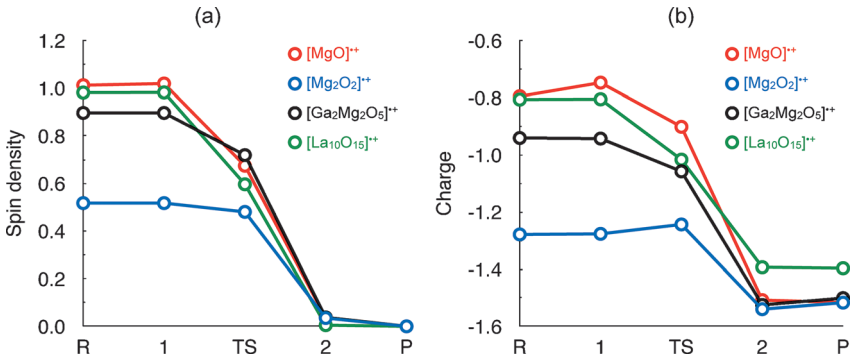

Figure 3. Evolution of the spin (a) and charge (b) densities at the bridging oxygen atom of the reactive sites in $[Mg_2O_2]^{\bullet+}$ (blue), $[Ga_2Mg_2O_5]^{\bullet+}$ (black), and $[La_{10}O_{15}]^{\bullet+}$ (green), and at the terminal oxygen in $[MgO]^{\bullet+}$ (red) along the reaction coordinates for HAT from methane.

In summary, this study shows that a bridging oxygen atom bearing an unpaired electron ($O_b^{\bullet-}$) as in $[Ga_2Mg_2O_5]^{\bullet+}$ corresponds to the reactive site for the C–H bond activation of methane and ethane. Insights from QC calculations not only deepen our understanding of C–H bond activation but also provide important guidance for the rational design of catalysts. To the best of our knowledge, hydrogen atom abstraction from CH_4 by $[Ga_2Mg_2O_5]^{\bullet+}$ constitutes the first example of the thermal activation of methane by a bridging-oxygen-bonded ($O_b^{\bullet-}$) binary element oxide cluster. The increased reactivity is due to a doping effect of the Ga_2O_3 unit on the otherwise inert cluster $[Mg_2O_2]^{\bullet+}$.

Keywords: C–H activation · computational chemistry · gas-phase reactions · mass spectrometry · radicals

How to cite: *Angew. Chem. Int. Ed.* **2015**, *54*, 5074–5078
Angew. Chem. **2015**, *127*, 5163–5167

[1] a) H. Schwarz, *Isr. J. Chem.* **2014**, *54*, 1413; b) H. Schwarz, *Angew. Chem. Int. Ed.* **2011**, *50*, 10096; *Angew. Chem.* **2011**, *123*, 10276; c) X.-L. Ding, X.-N. Wu, Y.-X. Zhao, S.-G. He, *Acc. Chem. Res.* **2012**, *45*, 382; d) D. Schröder, H. Schwarz, *Proc. Natl. Acad. Sci. USA* **2008**, *105*, 18114; e) R. H. Crabtree, *Chem. Rev.* **1995**, *95*, 2599.

[2] a) D. Schröder, *Angew. Chem. Int. Ed.* **2010**, *49*, 850; *Angew. Chem.* **2010**, *122*, 862; b) B. A. Arndtsen, R. G. Bergman, T. A. Mobley, T. H. Peterson, *Acc. Chem. Res.* **1995**, *28*, 154; c) H. Schwarz, *Angew. Chem. Int. Ed. Engl.* **1991**, *30*, 820; *Angew. Chem.* **1991**, *103*, 837.

[3] a) N. Dietl, M. Schlangen, H. Schwarz, *Angew. Chem. Int. Ed.* **2012**, *51*, 5544; *Angew. Chem.* **2012**, *124*, 5638; b) W. Lai, C. Li, H. Chen, S. Shaik, *Angew. Chem. Int. Ed.* **2012**, *51*, 5556; *Angew. Chem.* **2012**, *124*, 5652; c) X.-N. Wu, Y.-X. Zhao, W. Xue, Z.-C. Wang, S.-G. He, X.-L. Ding, *Phys. Chem. Chem. Phys.* **2010**, *12*, 3984.

[4] a) X.-N. Wu, X.-N. Li, X.-L. Ding, S.-G. He, *Angew. Chem. Int. Ed.* **2013**, *52*, 2444; *Angew. Chem.* **2013**, *125*, 2504; b) Z.-C. Wang, J.-W. Liu, M. Schlangen, T. Weiske, D. Schröder, J. Sauer, H. Schwarz, *Chem. Eur. J.* **2013**, *19*, 11496; c) Z. C. Wang, N. Dietl, R. Kretschmer, J. B. Ma, T. Weiske, M. Schlangen, H. Schwarz, *Angew. Chem. Int. Ed.* **2012**, *51*, 3703; *Angew. Chem.* **2012**, *124*, 3763; d) J.-B. Ma, Z.-C. Wang, M. Schlangen, S.-G. He, H. Schwarz, *Angew. Chem. Int. Ed.* **2012**, *51*, 5991; *Angew. Chem.* **2012**, *124*, 6093; e) Z.-C. Wang, T. Weiske, R. Kretschmer, M. Schlangen, M. Kaupp, H. Schwarz, *J. Am. Chem. Soc.* **2011**, *133*, 16930; f) N. Dietl, R. F. Höckendorf, M. Schlangen, M. Lerch, M. K. Beyer, H. Schwarz, *Angew. Chem. Int. Ed.* **2011**, *50*, 1430; *Angew. Chem.* **2011**, *123*, 1466; g) K. Chen, Z.-C. Wang, M. Schlangen, Y.-D. Wu, X. Zhang, H. Schwarz, *Chem. Eur. J.* **2011**, *17*, 9619; h) Y.-X. Zhao, X.-N. Wu, J.-B. Ma, S.-G. He, X.-L. Ding, *Phys. Chem. Chem. Phys.* **2011**, *13*, 1925; i) Z.-Y. Li, Y.-X. Zhao, X.-N. Wu, X.-L. Ding, S.-G. He, *Chem. Eur. J.* **2011**, *17*, 11728; j) J.-B. Ma, X.-N. Wu, X.-X. Zhao, X.-L. Ding, S.-G. He, *Phys. Chem. Chem. Phys.* **2010**, *12*, 12223; k) Y.-X. Zhao, X.-N. Wu, Z.-C. Wang, S.-G. He, X.-L. Ding, *Chem. Commun.* **2010**, *46*, 1736; l) X. Zhang, H. Schwarz, *ChemCatChem* **2010**, *2*, 1391; m) Z.-C. Wang, X.-N. Wu, Y.-X. Zhao, J.-B. Ma, X.-L. Ding, S.-G. He, *Chem. Phys.*

Lett. **2010**, *489*, 25; n) X.-L. Ding, Y.-X. Zhao, X.-N. Wu, Z.-C. Wang, J.-B. Ma, S.-G. He, *Chem. Eur. J.* **2010**, *16*, 11463; o) S. Feyel, J. Döbler, R. F. Höckendorf, M. K. Beyer, J. Sauer, H. Schwarz, *Angew. Chem. Int. Ed.* **2008**, *47*, 1946; *Angew. Chem.* **2008**, *120*, 1972; p) S. Feyel, J. Döbler, D. Schröder, J. Sauer, H. Schwarz, *Angew. Chem. Int. Ed.* **2006**, *45*, 4681; *Angew. Chem.* **2006**, *118*, 4797; q) D. Schröder, A. Fiedler, J. Hrušák, H. Schwarz, *J. Am. Chem. Soc.* **1992**, *114*, 1215.

[5] a) X.-N. Wu, B. Xu, J.-H. Meng, S.-G. He, *Int. J. Mass Spectrom.* **2012**, *310*, 57; b) X. N. Wu, X. L. Ding, S. M. Bai, B. Xu, S. G. He, Q. Shi, *J. Phys. Chem. C* **2011**, *115*, 13329.

[6] a) A. Oda, H. Torigoe, A. Itadani, T. Ohkubo, T. Yumura, H. Kobayashi, Y. Kuroda, *J. Phys. Chem. C* **2014**, *118*, 15234; b) C. Geng, S. Ye, F. Neese, *Dalton Trans.* **2014**, *43*, 6079; c) J. M. Mayer, *Acc. Chem. Res.* **2011**, *44*, 36.

[7] a) J. M. Mayer, *J. Phys. Chem. Lett.* **2011**, *2*, 1481; b) C. T. Saouma, J. M. Mayer, *Chem. Sci.* **2014**, *5*, 21.

[8] a) P. Schwach, M. G. Willinger, A. Trunschke, R. Schlögl, *Angew. Chem. Int. Ed.* **2013**, *52*, 11381; *Angew. Chem.* **2013**, *125*, 11591; b) K. Kwapien, M. Sierka, J. Döbler, J. Sauer, *ChemCatChem* **2010**, *2*, 819; c) V. García, J. J. Fernández, W. Ruíz, F. Mondragón, A. Moreno, *Catal. Commun.* **2009**, *11*, 240; d) R. Bouarab, O. Akdim, A. Auroux, O. Cherifi, C. Mirodatos, *Appl. Catal. A* **2004**, *264*, 161; e) C.-W. Hu, H.-Q. Yang, N.-B. Wong, Y.-Q. Chen, M.-C. Gong, A.-M. Tian, C. Li, W.-K. Li, *J. Phys. Chem. A* **2003**, *107*, 2316; f) R. H. Nibbelke, J. Scheerova, M. H. J. M. Decroon, G. B. Marin, *J. Catal.* **1995**, *156*, 106.

[9] D. Schröder, J. Roithová, *Angew. Chem. Int. Ed.* **2006**, *45*, 5705; *Angew. Chem.* **2006**, *118*, 5835.

[10] J. M. Recio, R. Pandey, A. Ayuela, A. B. Kunz, *J. Chem. Phys.* **1993**, *98*, 4783.

[11] K. Kwapien, J. Paier, J. Sauer, M. Geske, U. Zavyalova, R. Horn, P. Schwach, A. Trunschke, R. Schlögl, *Angew. Chem. Int. Ed.* **2014**, *53*, 8774; *Angew. Chem.* **2014**, *126*, 8919.

[12] a) P. Myrach, N. Nilius, S. V. Levchenko, A. Gonchar, T. Risse, K.-P. Dinse, L. A. Boatner, W. Frandsen, R. Horn, H.-J. Freund, R. Schlögl, M. Scheffler, *ChemCatChem* **2010**, *2*, 854; b) C. H. Lin, T. Ito, J. Wang, J. H. Lunsford, *J. Am. Chem. Soc.* **1987**, *109*, 4808.

[13] K. Kwapien, M. Sierka, J. Döbler, J. Sauer, M. Haertelt, A. Fielicke, G. Meijer, *Angew. Chem. Int. Ed.* **2011**, *50*, 1716; *Angew. Chem.* **2011**, *123*, 1754.

[14] P. Schwach, M. G. Willinger, A. Trunschke, R. Schlögl, *Angew. Chem. Int. Ed.* **2013**, *52*, 11381; *Angew. Chem.* **2013**, *125*, 11591.

[15] B. Chan, J. Deng, L. Radom, *J. Chem. Theory Comput.* **2011**, *7*, 112.

[16] G. S. Hammond, *J. Am. Chem. Soc.* **1955**, *77*, 334.

[17] R. F. W. Bader, *Atoms in Molecules: A Quantum Theory*, Oxford University Press, New York, **1994**.

[18] J. H. Meng, Y. X. Zhao, S. G. He, *J. Phys. Chem. C* **2013**, *117*, 17548.

Received: December 29, 2014
Published online: February 27, 2015

